Available online at www.sciencedirect.com
SCIENCE DIRECT®
PERGAMON
International Journal of Heat and Mass Transfer 46 (2003) 4823–4833
International Journal of HEAT and MASS TRANSFER
www.elsevier.com/locate/ijhmt

Low Reynolds number mixed convection in vertical tubes with uniform wall heat flux

A. Behzadmehr [a,b], N. Galanis [a,*], A. Laneville [a]

[a] *Génie mécanique, Université de Sherbrooke, Sherbrooke, QC, Canada J1K 2R1*
[b] *Mechanical Engineering, University of Sistan and Baluchestan, Zahedan, I.R. Iran*

Received 21 June 2002; received in revised form 27 May 2003

Abstract

Upward mixed convection of air in a long, vertical tube with uniform wall heat flux has been studied numerically for $Re = 1000$, $Re = 1500$ and $Gr \leqslant 10^8$ using a low Reynolds number k–ε model. The results for the fully developed region identify two critical Grashof numbers for each Reynolds number, which correspond to laminar–turbulent transition and relaminarization of the flow. They also distinguish the Re–Gr combinations that result in a pressure decrease over the tube length from those resulting in a pressure increase. A correlation expressing the fully developed Nusselt number in terms of the Grashof and Reynolds numbers is proposed. It is valid for laminar and turbulent flows in the range $1000 \leqslant Re \leqslant 1500$, $Gr \leqslant 5 \times 10^7$.

1. Introduction

Mixed convection in ducts occurs in many installations such as nuclear reactors, boilers, solar collectors and heat exchangers. It is therefore being studied extensively. An early article by Eckert and Diaguila [1] analyzed simultaneous free and forced convection in a short vertical tube. In 1989 Jackson et al. [2] presented a review of experimental and theoretical studies on mixed convection in vertical tubes. Some more recent publications are referred to in the present article.

Studies of heated ascending laminar flow in vertical and inclined tubes with $Re < 2000$ indicate that the Nusselt number for mixed convection, Nu_M, is larger than the corresponding value for forced convection, Nu_F [2–5]. On the other hand, for heated descending laminar flow with $Re < 2000$, Nu_M is smaller than Nu_F [2,4]. When the flow is turbulent the relationship between Nu_M and Nu_F is quite different [2,6–8]. Thus, for vertical tubes, when forced and free convection are in the same direction Nu_M is smaller than the corresponding Nu_F if the heating is weak and the mass flow rate relatively high (low values of the Richardson number and the buoyancy parameter). For high values of the Richardson number and the buoyancy parameter, Nu_M is larger than Nu_F. On the other hand, when forced and free convection are in opposite directions, Nu_M is always larger than Nu_F. For $Re > 2000$ relaminarization can occur and for these conditions Nu_M can be less than Nu_F [6,9]. This complicated behavior of Nu_M explains the lack of definitive information on this subject in heat transfer handbooks and textbooks. A further complication arises from the difficulty of deciding whether a given flow (defined by its Prandtl, Reynolds and Grashof numbers or by the dimensional quantities appearing in their expressions) is laminar or turbulent. Therefore, it is quite difficult to calculate the heat transfer coefficient for mixed convection flows.

Numerical studies of mixed convection in tubes with $Re > 2000$ have been carried out using different turbulent models [6,9,10] and have been successful in predicting the experimentally observed laminarization effects of the buoyancy force. On the other hand, all numerical studies for $Re < 2000$ have used the laminar

* Corresponding author. Tel.: +1-819-821-7144; fax: +1-819-821-7163.
E-mail address: nicolas.galanis@gme.usherb.ca (N. Galanis).

0017-9310/$ - see front matter © 2003 Elsevier Ltd. All rights reserved.
doi:10.1016/S0017-9310(03)00323-5

Nomenclature

Bo	buoyancy parameter $8\times10^4\ Gr\,Re^{-3.425}\,Pr^{-0.8}$
C_p	specific heat
D	internal tube diameter
G	turbulent production
g	acceleration of gravity
Gr	Grashof number $g\beta D^4 q_w/\lambda\nu^2$
I	turbulent intensity
k	turbulent kinetic energy
L	tube length
n	normal to the wall
Nu	Nusselt number $q_w D/\lambda(T_w-T_B)$
p	time averaged pressure
Pr	Prandtl number $\mu C_p/\lambda$
q_w	uniform heat flux at the solid–fluid interface
r	radial coordinate
Re	Reynolds number $U_0 D/\nu$
T, t	time averaged and fluctuating temperature
U, u	time averaged and fluctuating velocity
Z	axial coordinate

Greek symbols

β	volumetric expansion coefficient
Δp	pressure difference between the tube inlet and outlet
ε	dissipation of turbulent kinetic energy
θ	tangential coordinate
λ	thermal conductivity
μ, ν	dynamic, kinematic viscosity
ρ	density

Subscripts

B	bulk
F	forced convection
i, j	tensor index
L	outlet conditions
M	mixed convection
0	inlet condition
w	wall
r, z, θ	radial, axial, tangential direction

equations [3–5]. Nevertheless, experimental evidence compiled by Metais and Eckert [11] indicates that mixed convection in tubes can be turbulent for Reynolds numbers as low as 1000. Therefore, the laminar model is of limited practical interest since it can only handle the simplest flow conditions. In view of these observations, it is preferable to use turbulent models with a proven capability of predicting laminar flow fields for the analysis of convection heat transfer. The low Reynolds number k–ε models are among the primary candidates for such analyses. Indeed, Jones and Launder [12] have shown that in some cases turbulent solutions for such a model do not exist for accelerating flows. They state, "if one starts the predictions with an initially turbulent boundary layer and then applies the acceleration, the turbulence gradually decays away and the mean velocity profile collapses to that appropriate to laminar flow". A slightly different version of this model has in fact been used [6] to study developing mixed convection for $Re = 5000$, $Pr = 0.7$ and different Grashof numbers. However, as far as we can ascertain, such a model has never been used for mixed convection with $Re < 2000$.

In view of this situation, our research which has previously focused on laminar mixed convection [5,13,14], presently uses the Launder and Sharma low Reynolds number k–ε model [15] to study ascending mixed convection with $Re < 2000$. The methodology and objectives are similar to those of some recent numerical studies of confined forced flows with strong heating [16,17]. Earlier [18], we discussed flow reversal patterns for upward mixed convection in a vertical tube with $Pr = 0.7$, $Re = 1000$ and three Grashof numbers. These fully developed fields were all laminar. In the present article both laminar and turbulent fully developed fields are considered. Pressure, temperature and velocity distributions for $Pr = 0.7$, $Re = 1000$ and $Re = 1500$ over a wide range of Grashof numbers ($Gr \leqslant 10^8$) are presented. The specific aims of this paper are:

- To establish the transition conditions between laminar and turbulent conditions in terms of critical Grashof numbers for each Reynolds number.
- To investigate the relationship between different Re–Gr combinations and the pressure difference between the tube inlet and outlet.
- To obtain a correlation of the Nusselt number in terms of the Grashof and Reynolds numbers, valid for both laminar and turbulent flows.

2. Mathematical formulation and numerical procedure

We consider upward flow in a long vertical tube with uniform wall heat flux at the fluid–solid interface. The fluid properties are assumed constant except for the density in the body force, which varies linearly with temperature. Dissipation and pressure work are neglected as in all studies cited earlier. Therefore, the dimensional equations for steady state mean conditions are

$$\frac{\partial U_j}{\partial X_j} = 0 \tag{1}$$

$$\rho \frac{\partial}{\partial X_j}(U_j U_i) = \frac{-\partial P}{\partial X_i} + \frac{\partial}{\partial X_j}\left[\mu\left(\frac{\partial U_i}{\partial X_j} + \frac{\partial U_j}{\partial X_i}\right) - \rho\overline{u_i u_j}\right] + [1 - \beta(T - T_0)]\rho g_i \tag{2}$$

$$\rho \frac{\partial}{\partial X_j}\left(C_p U_j \frac{\partial T}{\partial X_j}\right) = \frac{\partial}{\partial X_j}\left[\lambda \frac{\partial T}{\partial X_j} - C_p \rho \overline{u_j t}\right] \tag{3}$$

In cylindrical coordinates:

$$X_1 = r, \quad X_2 = \theta, \quad X_3 = Z \tag{4a}$$

For Z positive in the flow direction,

$$g_1 = g_2 = 0 \quad \text{and} \quad g_3 = -g \tag{4b}$$

Turbulence is modeled with the Launder and Sharma [15] low Reynolds number k–ε model which gives accurate predictions for intermediate Reynolds numbers and for boundary layers with adverse pressure gradients [19]. It has been used successfully to model turbulent mixed convection for $Re \geqslant 2100$ [6] and is expressed by the following relations:

$$\frac{\partial}{\partial X_j}(U_j k) = \frac{\partial}{\partial X_j}\left[\left(\nu + \frac{\nu_t}{\sigma_k}\right)\frac{\partial k}{\partial X_j}\right] + G_k + G_b - \varepsilon - 2\nu\left(\frac{\partial \sqrt{k}}{\partial X_j}\right)^2 \tag{5}$$

$$\frac{\partial}{\partial X_j}(U_j \varepsilon) = \frac{\partial}{\partial X_j}\left[\left(\nu + \frac{\nu_t}{\sigma_\varepsilon}\right)\frac{\partial \varepsilon}{\partial X_j}\right] + c_1 f_1 \frac{\varepsilon}{k}(G_k + G_b) - c_2 f_2 \frac{\varepsilon^2}{k} + 2\nu\nu_t\left(\frac{\partial^2 U_i}{\partial X_j \partial X_k}\right)^2 \tag{6}$$

where

$$G_k = -\overline{u_i u_j}\frac{\partial U_i}{\partial X_j}, \quad G_b = -\frac{\beta}{\rho} g_i \overline{u_i t} = g_i \frac{\beta}{\rho}\frac{\nu_t}{Pr_t}\frac{\partial T}{\partial X_i},$$

$$\nu_t = c_\mu f_\mu \frac{k^2}{\varepsilon}$$

$$c_1 = 1.44, \quad c_2 = 1.92, \quad c_\mu = 0.09, \quad f_1 = 1, \quad Pr_t = 0.9,$$

$$\sigma_k = 1, \quad \sigma_\varepsilon = 1.3$$

$$f_2 = 1 - 0.3\exp(-R_t^2), \quad f_\mu = \exp\left[\frac{-3.4}{(1 + R_t/50)^2}\right],$$

$$R_t = \frac{k^2}{\nu\varepsilon} \tag{7}$$

It should be noted that no assumption of symmetry is introduced (field variables vary with all three space coordinates). These equations have been presented in cylindrical coordinates with the boundary layer approximation [6] and for fully developed flow [10]. The present study does not use either of these simplifications.

The boundary conditions areas follows:

At the tube entrance $(Z = 0)$: $U_z = U_0, \quad U_\theta = U_r = 0, \quad T = T_0, \quad I = I_0$ (8a)

Since the adopted model incorporates the assumption of turbulence isotropy, the corresponding turbulent kinetic energy is $k_0 = 1.5(I_0 U_0)^2$ (8b)

At the tube outlet $(Z = L)$: All axial derivatives are zero (9)

At the fluid–solid interface $(r = D/2)$:

$$U_i = 0, \quad k = \varepsilon = 0, \quad q_w = -\lambda\frac{\partial T}{\partial n} \tag{10}$$

This set of coupled non-linear differential equations was discretized with the control volume technique. For the convective and diffusive terms a second order upwind method was used while the SIMPLEC procedure was introduced for the velocity–pressure coupling. The discretization grid is uniform in the circumferential direction and non-uniform in the other two directions. It is finer near the tube entrance and near the wall where the velocity and temperature gradients are large. Several different grid distributions have been tested to ensure that the calculated results are grid independent. Although none of these tests showed any variation in the circumferential direction we retained the three dimensional formulation for future applications. The selected grid consists of 220, 48 and 8 nodes in the axial, radial and circumferential directions respectively.

The computer code was validated by comparing its results with velocity and temperature measurements for laminar developing mixed convection [3] and for fully developed turbulent mixed convection [20]. As shown in Fig. 1 the agreement is satisfactory except for the laminar temperature profile near the tube entrance ($Z/Pe = 0.01496$ or $Z/D = 4$). However, as explained by the experimenters [3] the measured temperatures close to the tube entrance were influenced by upstream conduction through the tube walls. The numerical predictions of their laminar model [3] for the temperature profile at $Z/D \cong 4$ are very close to the numerical results in Fig. 1. Furthermore as shown in Fig. 2, the predicted laminar fully developed velocity and temperature profiles are in excellent agreement with the corresponding analytical solution by Hallman [21]. Therefore, the model and the numerical procedure are reliable and can be used for the analysis of both laminar and turbulent mixed convection.

3. Results and discussion

Results in this section illustrate the effect of the Grashof number on the flow characteristics. They have

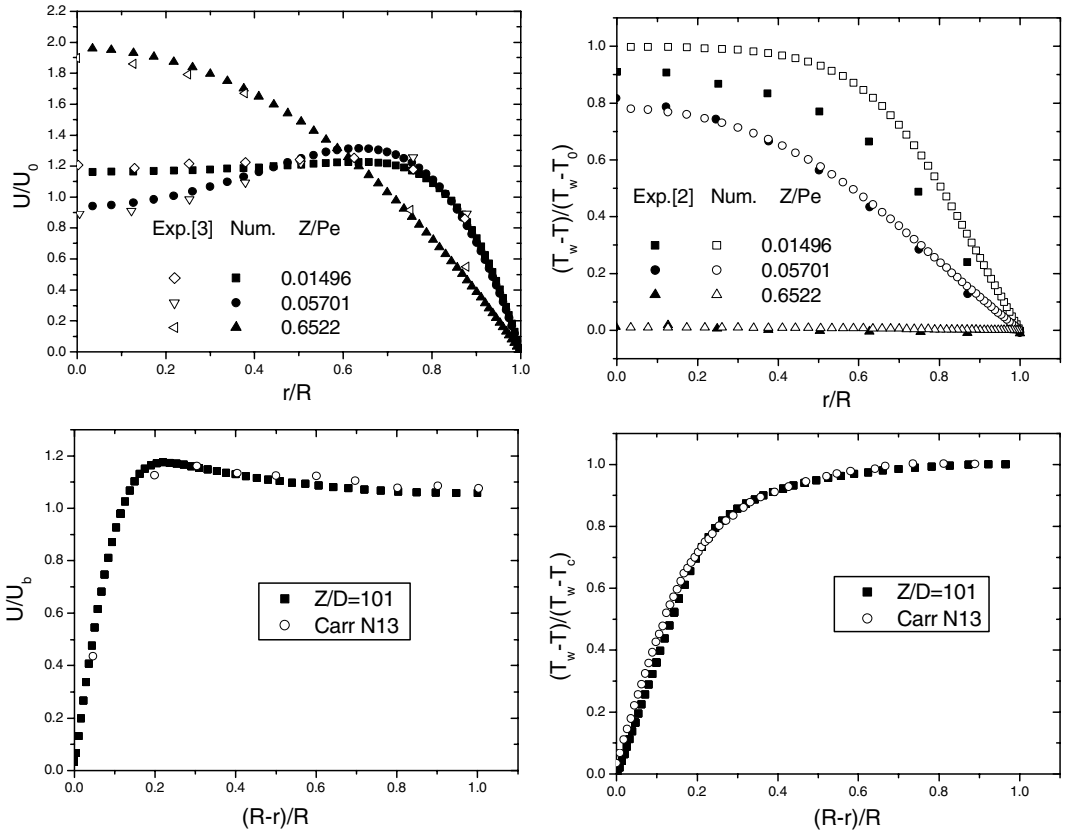

Fig. 1. Experimental validation for laminar and turbulent flow conditions.

been calculated using air as the fluid and $L = 101D$. The Prandtl number and the inlet turbulence intensity are constant at 0.71 and 0.1% respectively while the Reynolds number is equal to 1000 or 1500. The discussion focuses on the fully developed region whose existence has been established previously [22,23] by showing that the velocity profiles, the skin friction coefficient, the turbulent kinetic energy and the Nusselt number become independent of the axial position.

Fully developed turbulent kinetic energy profiles for four representative Grashof numbers are shown in Fig. 3. In order to put into perspective these values it should be noted that at the tube inlet $k/U_0^2 = 1.5 \times 10^{-6}$. For the lowest Grashof number ($Gr = 7 \times 10^5$) the fully developed turbulent kinetic energy is lower than this inlet value at all radial positions and for both Reynolds numbers. Therefore, for this Grashof number dissipation effects predominate over turbulence generation and the corresponding fully developed flow fields can be classified as laminar. When the Grashof number increases to 3×10^6, the fully developed values of the turbulent kinetic energy for $Re = 1500$ are considerably higher than its inlet value. For this *Re–Gr* combination, turbulence generation in the entrance region is stronger than dissipation and the corresponding fully developed flow field is turbulent. On the other hand, the fully developed flow field for $Re = 1000$, $Gr = 3 \times 10^6$ is still laminar. When the Grashof number increases further to 10^7 the fully developed flow field is turbulent for both Reynolds numbers. The critical value of Gr for transition from laminar to turbulent conditions is approximately 8×10^6 for $Re = 1000$ and 2×10^6 for $Re = 1500$. These values are quite close to the results in the Metais and Eckert chart [11]. Finally, for the highest Grashof number, $Gr = 7 \times 10^7$, the fully developed flow field is turbulent for $Re = 1500$ and laminar for $Re = 1000$. This second transition from turbulent to laminar conditions is due to the laminarization effect of the buoyancy-induced acceleration. Although this transition is not shown in the Metais and Eckert chart [11], its existence has been established for intermediate Reynolds numbers ($2000 < Re < 10000$) by both experimental and numerical studies [9,10]. The present one is the first to report this phenomenon for a Reynolds number less than 2000. The critical value of Gr for the relaminarization of turbulent flow is approximately 5×10^7 for $Re = 1000$ and 10^8 for $Re = 1500$.

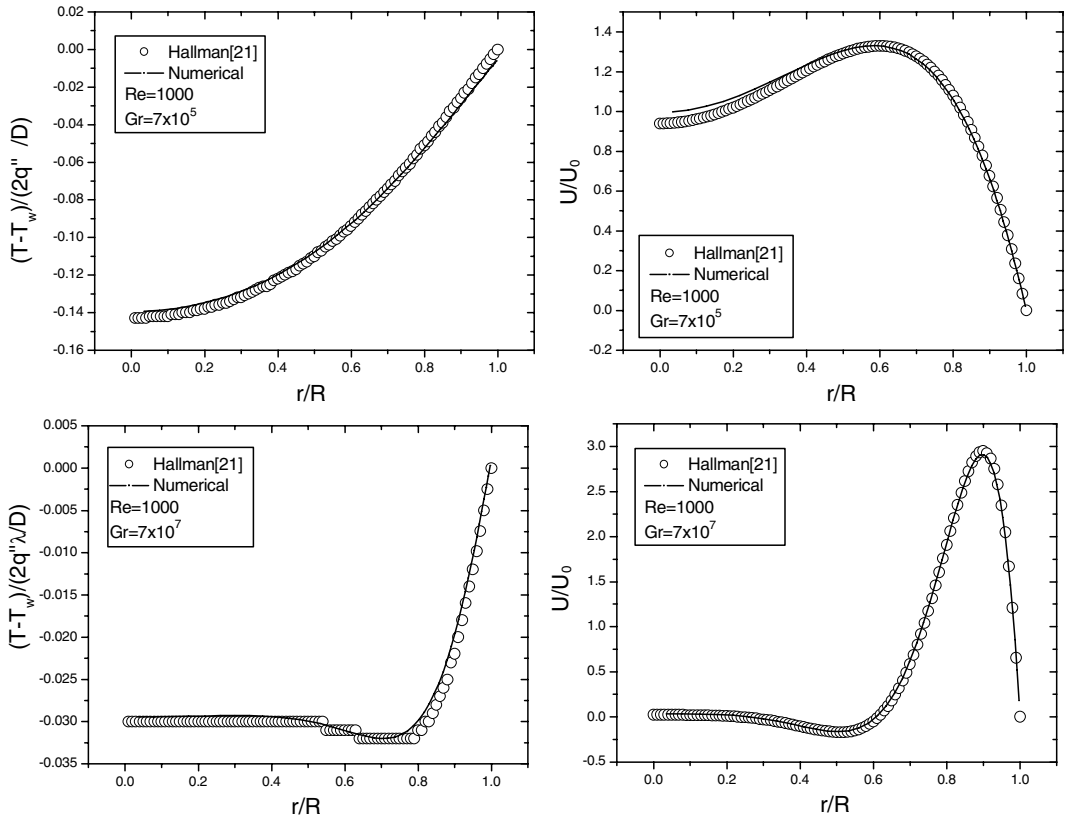

Fig. 2. Analytical validation for laminar fully developed conditions ($Re = 1000$).

It should be noted that, when the flow is turbulent for both Reynolds numbers (Fig. 3c) the non-dimensional turbulent kinetic energy is higher for the lower Reynolds number since the effects of natural convection are more important when the Richardson number is higher. Furthermore, for turbulent flows the effect of increased heating on the turbulent kinetic energy is illustrated by comparing Fig. 3b–d for the case of $Re = 1500$: they show that the turbulent kinetic energy increases as Gr increases. In either case (constant Gr or constant Re) the turbulent production that causes the difference between the profiles of Fig. 3 is due to both velocity and temperature gradients (terms G_k and G_b in Eq. (5)) since the velocity and temperature fields depend on both Gr and Re (see Figs. 2 and 3).

Fig. 4 shows the fully developed velocity profiles for the same Re–Gr combinations. In all cases the maximum velocity does not occur at the tube axis as is the case for forced convection. This is due to the buoyancy-induced acceleration, which is more important near the wall where the fluid is warmer. Since for a given Grashof number the effect of heating is more important when the Reynolds number is low, the difference between the maximum velocity and its value at $r = 0$ is in general higher for $Re = 1000$. The difference between the profiles corresponding to the same Grashof number is greatest when the flow field for $Re = 1000$ is laminar and the one for $Re = 1500$ is turbulent (Fig. 4b and d). On the other hand, for $Gr = 10^7$, when both flow fields are turbulent (Fig. 4c) the difference between the velocity profiles for $Re = 1000$ and $Re = 1500$ is very small. As expected, the profiles for turbulent conditions are quite uniform and the velocity is everywhere positive (ascending). On the other hand, the profiles for laminar conditions are very distorted and can include zones of flow reversal (negative velocities) when the heating is intense (Fig. 4b and d for $Re = 1000$). As illustrated earlier (Fig. 2), all the calculated laminar velocity profiles are in excellent agreement with the analytical solution for fully developed laminar mixed convection [21]. Two different patterns of flow reversal are illustrated in these figures: the first one, for $Gr = 3 \times 10^6$, includes the tube axis while the second, for $Gr = 7 \times 10^7$, occurs between the centreline and the wall. This second flow reversal pattern, which has been predicted analytically [21], has not been obtained numerically by any study using the laminar equations. A detailed discussion of these flow reversal patterns has been presented elsewhere [18].

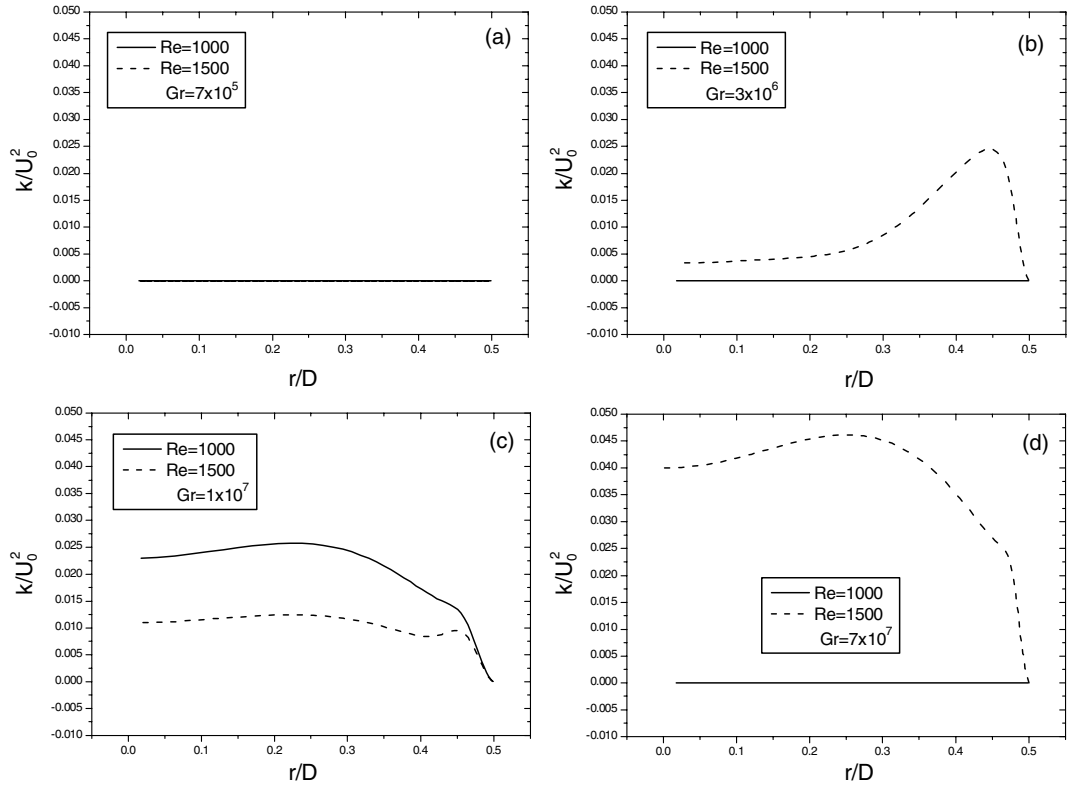

Fig. 3. Kinetic energy of turbulence in the fully developed region ($Pr = 0.71$, $I_0 = 0.1\%$, $Z/D = 98$).

Fig. 5 shows the radial distribution of the temperature increase between the tube inlet and the fully developed region ($Z = 98D$). As illustrated earlier (Fig. 3), all the calculated temperature profiles for laminar conditions are in agreement with the corresponding analytical solution by Hallman [21]. With the adopted non-dimensional formulation, the bulk temperature at a fixed axial position is inversely proportional to the Reynolds number and independent of the Grashof number. These properties of the solution are clearly reflected in Fig. 5. On the other hand, the radial distribution of this temperature difference depends on the hydrodynamic field. Thus, for the lowest Grashof number ($Gr = 7 \times 10^5$), for which the flow field is laminar for both Reynolds numbers, radial heat transfer takes place by conduction only. Therefore, this non-dimensional temperature at the wall is higher than for the other three values of Gr while the corresponding centreline temperature is the lowest. In fact, these results show that the non-dimensional wall temperature decreases monotonically as Gr increases. On the other hand, the corresponding centreline temperature increases monotonically as Gr increases. For $Gr = 3 \times 10^6$ the temperature difference between the wall and the centreline is lower when $Re = 1500$ since in that case the flow is turbulent and radial heat transfer is augmented by fluid mixing. For $Gr = 10^7$, when the flow is turbulent for both Reynolds numbers, the temperature variation is important near the wall and quite small in the core region. Finally, for the highest Grashof number ($Gr = 7 \times 10^7$), the temperature profiles for the two Reynolds numbers are quite similar. In both cases they consist of a thermal boundary layer with considerable temperature gradient and an essentially isothermal core. The reasons for these similar temperature distributions are however quite different. For $Re = 1500$ the flow is turbulent and, therefore, the core is thoroughly mixed, hence isothermal. On the other hand, for $Re = 1000$ the flow is laminar with very high axial velocity near $r = 0.45$ (Fig. 4d). Thus, most of the heat supplied to the fluid is carried downstream and a very small part is conducted radially towards the axis.

We now examine the distribution of the static pressure in the flow field. This variable is seldom analysed in mixed convection studies, contrary to the case of isothermal flow, despite the fact that it is extremely important for engineering applications and flow characterisation. Fig. 6 shows that its radial variation is negligible. On the other hand, for the conditions of this figure ($Re = 1000$, $Gr = 7 \times 10^4$) the pressure decreases significantly in the flow direction. The non-dimensional

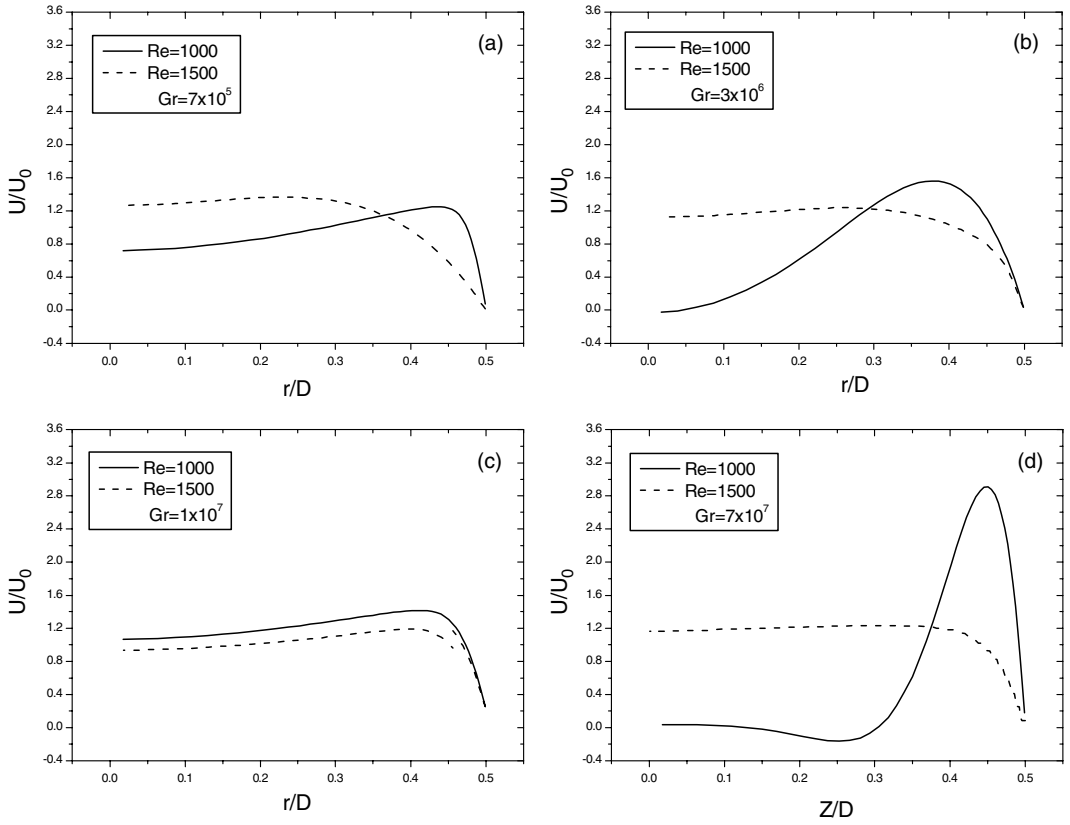

Fig. 4. Axial velocity profiles in the fully developed region ($Pr = 0.71$, $I_0 = 0.1\%$, $Z/D = 98$).

axial pressure drop over a tube length of 100 diameters is approximately 3.9. This is considerably lower than 6.4, which is the corresponding pressure drop for fully developed isothermal flow with the same Reynolds number. The reason for this significant reduction of the pressure drop (which corresponds to the imposed pressure difference, $\Delta p = p_0 - p_L$) is due to the heating of the fluid which facilitates its upward movement.

If the Grashof number is increased beyond 7×10^4 while maintaining $Re = 1000$, the imposed pressure difference Δp will continue to decrease. Eventually, this quantity becomes negative; i.e., the static pressure at the tube outlet becomes higher than the corresponding value at its inlet. This result, which has been confirmed experimentally [24] and has also been reported by Lawrence and Chato [25], is illustrated in Fig. 7 for both laminar and turbulent conditions. It is due to the fact that, when Gr increases due to the increase of q_w, the buoyancy-induced upward motion becomes progressively more significant. Therefore the imposed pressure difference must eventually be reversed to limit the mass flow rate to the value corresponding to the fixed Reynolds number. Thus, for example, the natural convection flow for $Gr = 10^7$ gives rise to a mass flow rate which corresponds to $Re > 1500$. In order to reduce it to 1500 or 1000, the pressure at the tube outlet must be higher than at its inlet. In other words, the imposed pressure difference Δp must be reversed to compensate for the increasing effect of the buoyancy force. This change from positive to negative values of Δp occurs approximately at $Gr = 3 \times 10^5$ for $Re = 1000$ and at $Gr = 4 \times 10^5$ for $Re = 1500$. These values and the results of Fig. 7 are consistent with the fact that the effects of buoyancy are more important for low Reynolds numbers. Since in all the cases examined here the mixed convection flow is upwards, those with $\Delta p > 0$ are flows with aiding pressure difference while those with $\Delta p < 0$ are flows with opposing pressure difference.

Fig. 8 shows the effect of the Grashof number on the calculated Nusselt number in the fully developed region. Fig. 8a and b, respectively for $Re = 1000$ and $Re = 1500$, also identify the conditions for laminar or turbulent regimes as well as those for positive or negative pressure differences between the tube inlet and outlet. For laminar condition these figures show that the fully developed Nusselt number increases slowly with Gr. For Grashof numbers beyond the first critical value ($Gr = 8 \times 10^6$ for

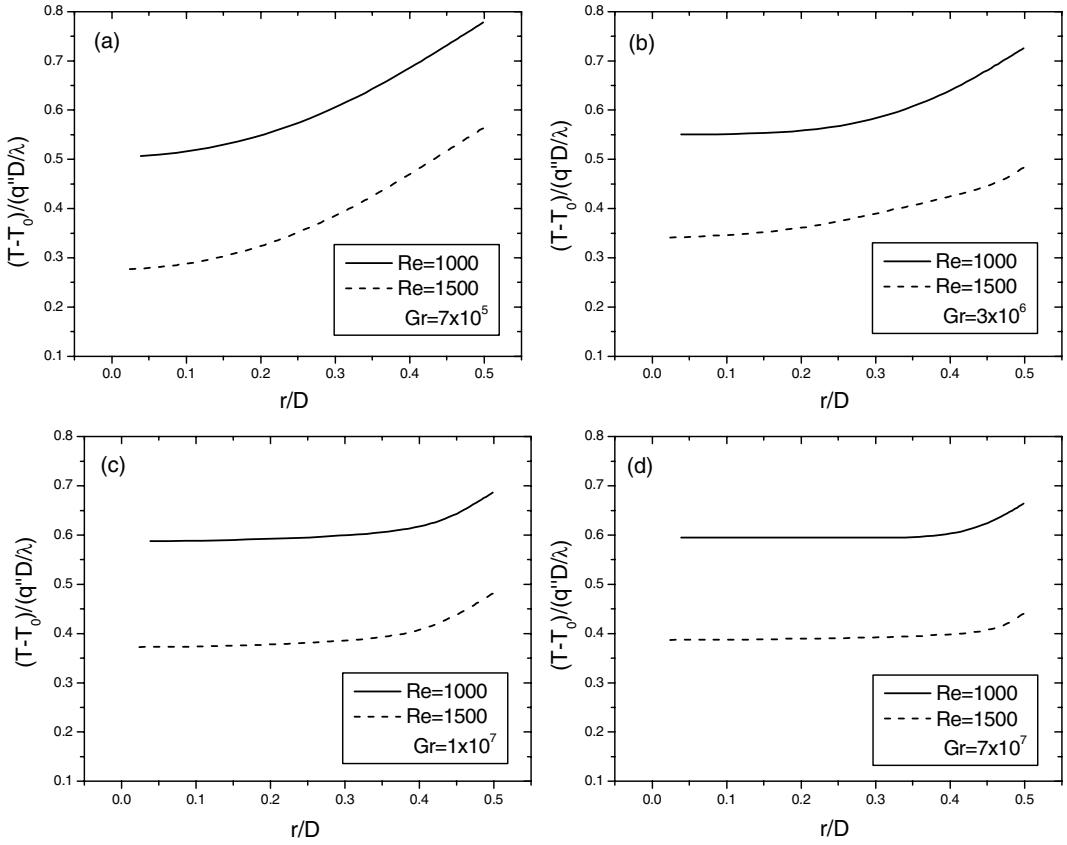

Fig. 5. Temperature profiles in the fully developed region ($Pr = 0.71$, $I_0 = 0.1\%$, $Z/D = 98$).

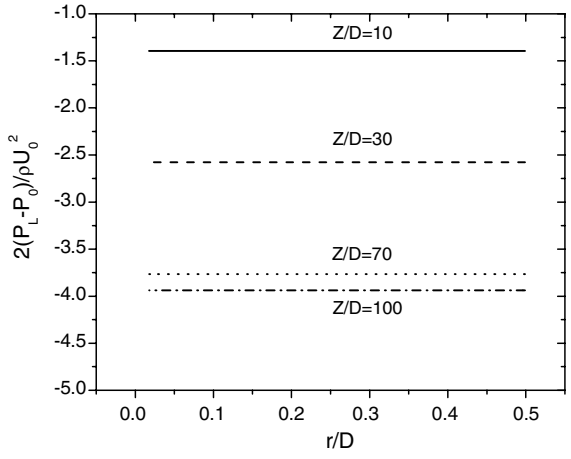

Fig. 6. Radial pressure distribution at different axial positions ($Pr = 0.71$, $Re = 1000$, $Gr = 7 \times 10^4$, $I_0 = 0.1\%$).

$Re = 1000$ and $Gr = 2 \times 10^6$ for $Re = 1500$), the fully developed flow field is turbulent and, as illustrated in Fig. 5c, the temperature difference between the wall and the fluid decreases due to mixing. Therefore the Nusselt number increases more rapidly than for laminar conditions as Gr increases towards the second critical value corresponding to the relaminarization of flow ($Gr = 5 \times 10^7$ for $Re = 1000$ and $Gr = 10^8$ for $Re = 1500$). For Grashof numbers higher than the second critical value, the effects of laminarization cause a decrease of Nu_M as reported and discussed in earlier studies [9,10] conducted with much higher Reynolds numbers.

These effects of Gr and Re on Nu_M can be expressed by the following correlation which, as shown in Fig. 8, represents accurately all the numerical results for $Gr \leqslant 5 \times 10^7$:

$$Nu_M = 4.36\left(1 + \frac{Gr^{0.468}}{750 + 0.24Re}\right) \tag{11}$$

This correlation is valid for fully developed upward mixed convection in vertical tubes with uniform wall heat flux for both laminar and turbulent conditions and for $1000 \leqslant Re \leqslant 1500$.

Fig. 9 shows that for laminar flow with opposing pressure difference ($P_0 < P_L$) the proposed correlation (Eq. (11)) agrees well with corresponding experimental

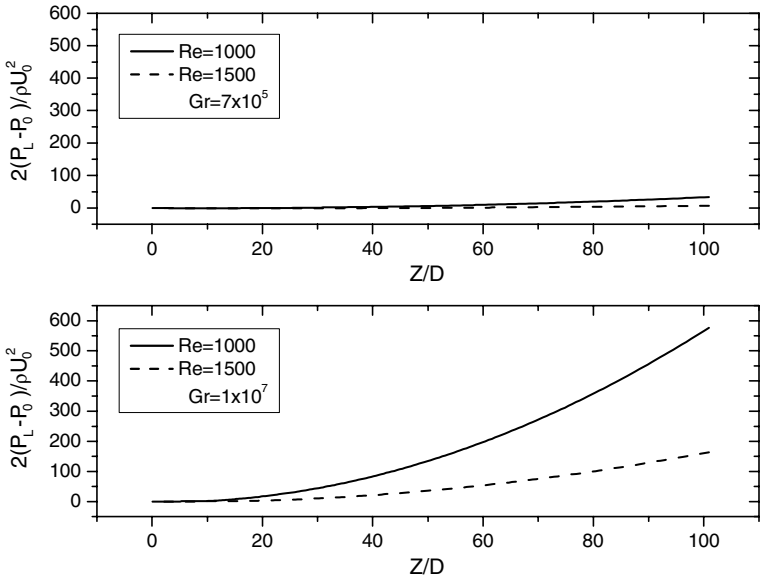

Fig. 7. Axial evolution of the static pressure ($Pr = 0.71$, $I_0 = 0.1\%$).

results [26] and the predictions of the following correlation:

$$Nu_M = 0.95(Gr/Re)^{0.28} \quad (12)$$

which has been proposed [2] for heated ascending laminar mixed convection with $100 < Gr/Re < 10\,000$. On the other hand, for laminar flow with $P_0 > P_L$ the difference between the values predicted from Eqs. (11) and (12) increases as Gr decreases. Thus, for $Re = 1000$ and $Gr = 10^5$ the numerical prediction is $Nu_M = 5.43$, while Eqs. (11) and (12) give $Nu_M = 5.38$ and $Nu_M = 3.45$ respectively. However, all studies of heated ascending laminar flow in vertical tubes with $Re < 2000$ indicate that Nu_M is larger than the corresponding value for forced convection [2–5]. Therefore for low values of Gr our numerical results and the predictions of Eq. (11) are more plausible than the prediction of Eq. (12). In particular, Eq. (11) predicts the correct value for Nu_M as $Gr \to 0$. For Grashof numbers beyond the first critical value, corresponding to laminar–turbulent transition, the values of Nu_M predicted by Eq. (12) cannot be compared with previously published values since, to the best of our knowledge, these are the first reported results for turbulent mixed convection with $Re < 2000$. Correlations such as those by Cotton and Jackson [6], Celata et al. [7] or Metais and Eckert [11] are based on flows with higher Reynolds numbers and give very different results from these in Fig. 8 when applied for the Re–Gr combination under consideration here.

It should be noted, that for Grashof values higher than the second critical value, the values of Nu_M in Fig. 8 cannot be compared with those calculated from Eq. (12) or from similar laminar correlations [11] since these correlations have been obtained for much lower heat fluxes (or, equivalently, Grashof numbers) than the ones leading to relaminarization.

Finally, Fig. 9 also shows that for the range of parameters under consideration, Nu_M increases slightly as Re decreases. This observation is consistent with the fact that the effects of a great heat flux are more important when the flow rate is lower (see, for example, Fig. 3c) and is in agreement with both Eq. (12) and Hallman's experimental results [26].

4. Conclusion

A study of upward mixed convection of air in a long vertical tube with uniform wall heat flux has been conducted for two very low Reynolds numbers ($Re = 1000$ and $Re = 1500$) over a wide range of Grashof numbers ($Gr \leqslant 10^8$) using a low Reynolds number k–ε model with proven capabilities of accurately simulating both laminar and turbulent flows. The results in the fully developed region define three critical Grashof numbers for each Reynolds number. The smallest critical value distinguishes the Re–Gr combinations that lead to a pressure decrease over the tube length from those leading to a pressure increase. The middle one corresponds to transition from laminar to turbulent conditions while the largest indicates the conditions for which relaminarization takes place. These three values are:

- 4×10^5, 8×10^6 and 5×10^7 for $Re = 1000$;
- 3×10^5, 2×10^6 and 10^8 for $Re = 1500$.

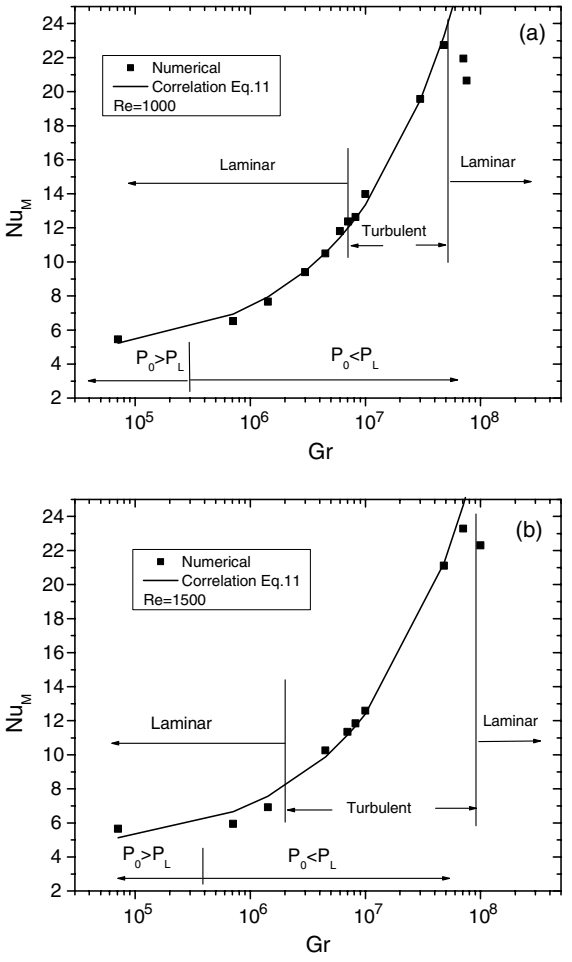

Fig. 8. Calculated and new correlation values of the Nusselt number in the fully developed region ($Pr = 0.71$, $I_0 = 0.1\%$).

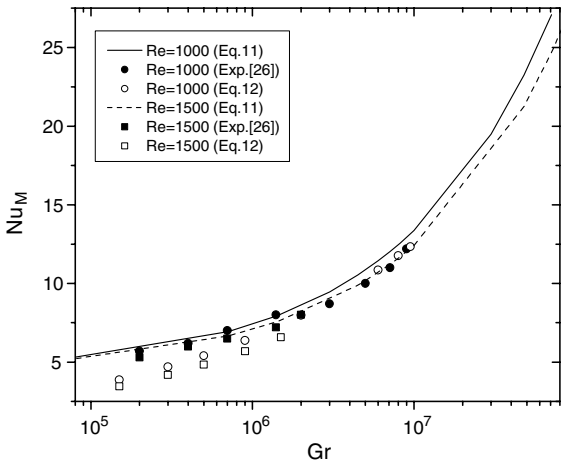

Fig. 9. Comparison of proposed correlation with previous results.

A correlation expressing the fully developed Nusselt number in terms of the Grashof number has been proposed. It is valid for $1000 \leqslant Re \leqslant 1500$, $Gr \leqslant 5 \times 10^7$ and laminar as well as turbulent flows in this range of parameters.

Acknowledgements

The authors thank the Natural Sciences and Engineering Research Council of Canada for its financial support as well as the Ministry of Science, Research and Technology of the I. R. Iran for the scholarship awarded to the first author.

References

[1] E.R.G. Eckert, A.J. Diaguila, Convective heat transfer for mixed, free, and forced flow through tubes, ASME Trans. 76 (1954) 497–504.
[2] J.D. Jackson, M.A. Cotton, B.P. Axcell, Studies of mixed convection in vertical tubes, Int. J. Heat Fluid Flow 10 (1) (1989) 2–15.
[3] B. Zeldin, F.W. Schmidt, Developing flow with combined forced-free convection in an isothermal vertical tube, ASME J. Heat Transfer 94 (1972) 211–223.
[4] M. Wang, T. Tsuji, Y. Nagano, Mixed convection with flow reversal in the thermal entrance region of horizontal and vertical pipes, Int. J. Heat Mass Transfer 37 (15) (1994) 2305–2319.
[5] M. Ouzzane, N. Galanis, Effets de la conduction pariétale et de la répartition du flux thermique sur la convection mixte près de l'entrée d'une conduite inclinée, Int. J. Therm. Sci. 38 (1999) 622–633.
[6] M.A. Cotton, J.D. Jackson, Vertical tube air flows in the turbulent mixed convection region calculated using a low-Reynolds-number k–ε model, Int. J. Heat Mass Transfer 33 (2) (1990) 275–286.
[7] G.P. Celata, F. D'Annibale, A. Chiaradia, M. Cumo, Upflow turbulent mixed convection heat transfer in vertical pipes, Int. J. Heat Mass Transfer 41 (1998) 4037–4054.
[8] P. Poskas, Turbulent mixed convection in channels for different orientations of them in space, J. Int. Eng. Phys. Thermophys. 69 (6) (1996) 738–746.
[9] H. Tanaka, S. Marugama, S. Hatano, Combined forced and natural convection heat transfer for upward flow in a uniformly heated vertical pipe, Int. J. Heat Mass Transfer 30 (1) (1987) 165–174.
[10] W.B. Hall, J.D. Jackson, Laminarization of a turbulent pipe flow by buoyancy forces, ASME Paper (96-HT-55), 1969.
[11] B. Metais, E.R.G. Eckert, Forced, mixed, and free convection regimes, ASME J. Heat Transfer 86 (1964) 295–296.
[12] W.P. Jones, B.E. Launder, The prediction of laminarization with a two-equation model of turbulence, Int. J. Heat Mass Transfer 15 (1972) 301–314.

[13] H. Nesreddine, N. Galanis, C.T. Nguyen, Effects of axial diffusion on laminar heat transfer with low péclet numbers in the entrance region of thin vertical tubes, Num. Heat Transfer, Part A 33 (1998) 247–266.
[14] J. Orfi, N. Galanis, C.T. Nguyen, Bifurcation in steady laminar mixed convection flow in uniformly heated inclined tubes, Int. J. Num. Methods Heat Fluid Flow 9 (1999) 543–567.
[15] B.E. Launder, B.I. Sharma, Application of the energy dissipation model of turbulence to the calculation of flow ear a spinning disc, Lett. Heat Mass Transfer 1 (1974) 131–138.
[16] K. Ezato, A.M. Shehata, T. Kunugi, D.M. McEligot, Numerical prediction of transitional features of turbulent forced gas flows in circular tubes with strong heating, ASME J. Heat Transfer 121 (1999) 546–555.
[17] S. Torii, W.J. Yang, Thermal-fluid transport phenomena in strongly heated channel flows, Int. J. Num. Methods Heat Fluid Flow 10 (8) (2000) 802–823.
[18] A. Behzadmehr, N. Galanis, A. Laneville, Flow reversal in laminar mixed convection, in: Proceeding of the ASME International Mechanical Engineering Congress and Exposition, Paper No. HTD-24111, New York, 2001.
[19] W.P. Jones, B.E. Launder, The calculation of low-Reynolds-number phenomena with a two-equation model of turbulence, Int. J. Heat Mass Transfer 16 (1973) 1119–1129.
[20] A.P. Carr, M.A. Connor, H.D. Buhr, Velocity, temperature, and turbulence measurements in air flow pipe flow with combined free and forced convection, ASME J. Heat Transfer 94 (1973) 211–223.
[21] T.M. Hallman, Combined forced and free laminar heat transfer in vertical tubes with uniform internal heat generation, ASME Trans. (1956) 1831–1841.
[22] A. Behzadmehr, N. Galanis, A. Laneville, Numerical analysis of laminar and turbulent flow regimes in developing mixed convection, in: Proceedings 12th International Heat Transfer Conference, Vol. 2, Grenoble, France, 2002, pp. 225–230.
[23] A. Behzadmehr, N. Galanis, A. Laneville, Laminar–turbulent transition for low Reynolds number mixed convection in a uniformly heated vertical tube, Int. J. Num. Methods Heat Fluid Flow 12 (7) (2002) 839–854.
[24] A. Behzadmehr, Étude numérique et expérimentale du phénomène de la transition en convection mixte dans le cas d'un tube vertical pour un nombre de Reynolds inférieur à 2000, Ph.D. thesis, Université de Sherbrooke, Sherbrooke QC, Canada, 2003.
[25] W.T. Lawrence, J.C. Chato, Heat transfer effects on the developing laminar flow inside vertical tubes, ASME J. Heat Transfer (1966) 214–222.
[26] T.M. Hallman, Experimental study of combined forced and free laminar convection in a vertical tube, NASA T.N. D-1104, 1961.